

## Electron Paramagnetic Resonance Studies of the Iron–Sulfur Centers from Complex I of *Rhodothermus marinus*<sup>†</sup>

Andreia S. Fernandes,<sup>‡,§</sup> Filipa L. Sousa,<sup>‡</sup> Miguel Teixeira,<sup>‡</sup> and Manuela M. Pereira<sup>\*,‡</sup>

Instituto de Tecnologia Química e Biológica, Universidade Nova de Lisboa, Av. da República, Apartado 127, 2784-505 Oeiras, Portugal, and Faculdade de Ciências e Tecnologia, Universidade do Algarve, Campus de Gambelas, 8005-139 Faro, Portugal

Received September 27, 2005; Revised Manuscript Received November 15, 2005

**ABSTRACT:** *Rhodothermus marinus*, a thermohalophilic Gram negative bacterium, contains a type I NADH/quinone oxidoreductase (complex I). Its purification was optimized, yielding large amounts of pure and active protein. Furthermore, the stoichiometry of NADH oxidation and quinone reduction was shown to be 1:1. The large amounts of protein enabled a thorough characterization by electron paramagnetic resonance (EPR) spectroscopy at different temperatures and microwave powers, using NADH, NADPH, and dithionite as reducing agents. A minimum of two  $[2\text{Fe-2S}]^{2+/1+}$  and four  $[4\text{Fe-4S}]^{2+/1+}$  centers were observed in the purified complex. Redox titrations monitored by EPR spectroscopy made possible the determination of the reduction potentials of the iron–sulfur centers; with the exception of one of the  $[4\text{Fe-4S}]^{2+/1+}$  centers, which has a lower reduction potential, all the other centers have reduction potentials of  $-240 \pm 20$  mV, pH 7.5.

Complex I of aerobic respiratory chains catalyzes the NADH:quinone oxidoreductase reaction coupled to charge translocation across the membrane, which contributes to the membrane electrochemical potential that is the driving force for ATP synthesis. The bovine complex is composed of more than 40 subunits and has a molecular mass of  $\sim 1$  MDa, while the bacterial counterpart is formed generally by 13 or 14 subunits (named *nqo1* to 14 or *nuoA* to N) with  $\sim 500$  kDa, the so-called minimal functional unit. Models of three-dimensional (3D) structures obtained at low resolution by negative staining electron microscopy or cryo-electron microscopy have revealed an L-shaped structure, with a membrane and a peripheral arm (1–5). The peripheral part contains a series of iron–sulfur centers (binuclear and tetranuclear) and noncovalently bound FMN and catalyzes NADH oxidation. Recently, by X-ray analysis (6), the iron–sulfur centers have been identified in a subcomplex, corresponding to the peripheral arm of *Thermus thermophilus* complex I. The mechanism of quinone reduction and its coupling to charge translocation is not known, and it is accepted that it occurs in the membrane part of the complex.

Eight canonical iron–sulfur center binding sites are present in the amino acid sequences of complex I subunits; depending on the organism, up to two more binding sites may be observed. All of them are located in the subunits of the peripheral arm or at the connecting domain. However, until now, only five or six iron–sulfur centers have been detected

by electron paramagnetic resonance (EPR)<sup>1</sup> in an intact complex; the other centers were detected only in individually expressed subunits. These centers are named N1a, N1b, N2, N3, N4, N5, N6a, and N6b. There is no consistent rule for this nomenclature, although Ohnishi (7) relates it with the spin relaxation of the center: the higher the center numbering, the faster is its spin relaxation and consequently the lower is the optimal temperature for its observation by EPR spectroscopy. Centers N1a and b are  $[2\text{Fe-2S}]^{2+/1+}$  centers, which relax more slowly and are detected even at liquid nitrogen temperature (at above 77 K), and all the others are  $[4\text{Fe-4S}]^{2+/1+}$  centers, which are detected below 20 K. In the case of complex I from *Escherichia coli* and *T. thermophilus*, a ninth iron–sulfur center was observed. It was recently shown to be a  $[4\text{Fe-4S}]^{2+/1+}$  center (8) and was named N7 (8, 9). In the arrangement of the nine iron–sulfur centers from complex I of *T. thermophilus* determined by X-ray analysis (6), seven of the centers are arranged in a continuous chain with edge-to-edge distances between 9 and of 14 Å. Centers N1a and N7 are not in this pathway.

Centers N1b, N3, N4, and N5 are usually referred as the isopotential group of iron–sulfur centers in complex I. With the exception of center N3 of *T. thermophilus* complex I, all other iron–sulfur centers reported until now have a reduction potential around  $-250$  mV (10–15). Center N1a has a low reduction potential between  $-420$  and  $-300$  mV, with the exception of the center from *Paracoccus denitrificans* complex I (10–13, 16). In mitochondria and related bacteria such as *P. denitrificans*, *Rhodobacter capsulatus*, and *Rhodobacter sphaeroides*, center N2 has the highest reduction potential in complex I, around  $-130$  mV, which

<sup>†</sup> This work was supported by Fundação para a Ciência e a Tecnologia (POCTI/BIA-PRO/58374/2004).

<sup>\*</sup> To whom correspondence should be addressed. Phone: 351-214469321. Fax: 351-214469314. E-mail: mpereira@itqb.unl.pt.

<sup>‡</sup> Universidade Nova de Lisboa.

<sup>§</sup> Universidade do Algarve.

<sup>1</sup> Abbreviations. DM, *n*-dodecyl  $\beta$ -D-maltoside; DMN, 2,3-dimethyl-1,4-naphthoquinone; EPR, electron paramagnetic resonance spectroscopy.

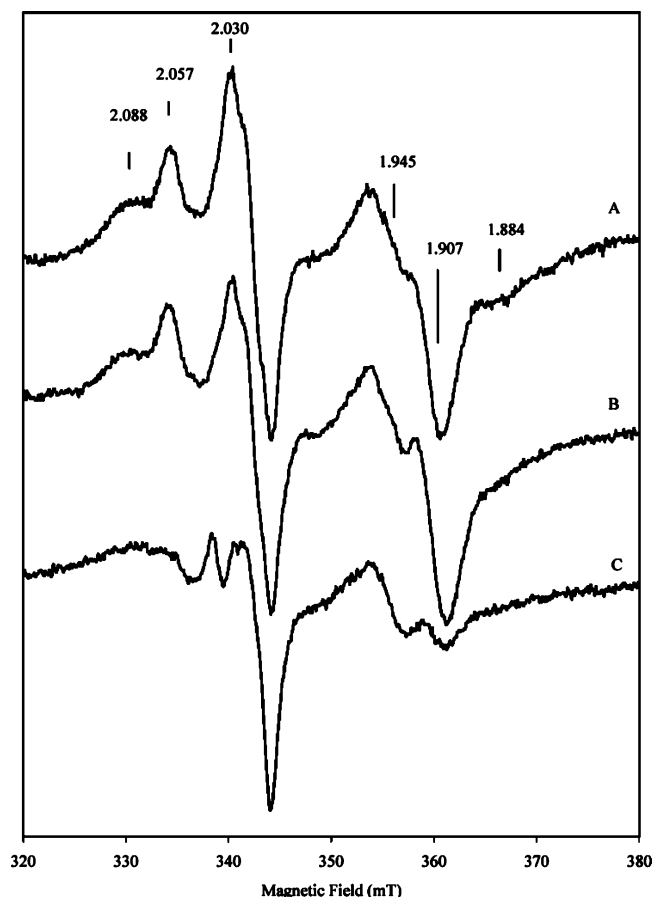


FIGURE 1: EPR spectra of *R. marinus* membranes at 2.4 mW, 10 K incubated with piericidin A and reduced with 10 mM NADH (A), NADPH (B), and succinate (C). Microwave frequency: 9.64 GHz; modulation amplitude: 0.9 mT.

is pH dependent (11, 13–16). In *T. thermophilus*, this value is pH independent and much lower,  $-304$  mV.

In the amino acid sequences of the subunits of *Rhodothermus marinus* complex I, a menaquinone-dependent enzyme, only the eight conserved iron–sulfur binding sites are present (17). A preliminary analysis of the iron–sulfur centers of *R. marinus* complex I was done previously (18). Two binuclear and three tetranuclear centers were observed by EPR spectroscopy of the purified complex. The quality of the spectra did not allow a safe conclusion about the presence of further centers. Now, the purification of *R. marinus* complex I has been optimized, and it was possible to obtain large amounts of protein to perform a more complete and accurate analysis of the iron–sulfur centers by EPR spectroscopy.

## METHODS

**Complex I Purification.** Bacterial growth was performed as described in ref 19, except that it was performed in a 10 L reactor and the growth medium contained 100 mM glutamate. Membrane preparation was done as described in ref 19. Protein purification was done as previously described (18) with the following modifications: the sample was passed through two successive high performance Q-Sepharose columns instead of a fast-flow Q-Sepharose and a chelating Sepharose; buffers were prepared at pH 8 (5 °C); EDTA was absent from the buffers. The three purification steps were done in three successive days without freezing the samples.

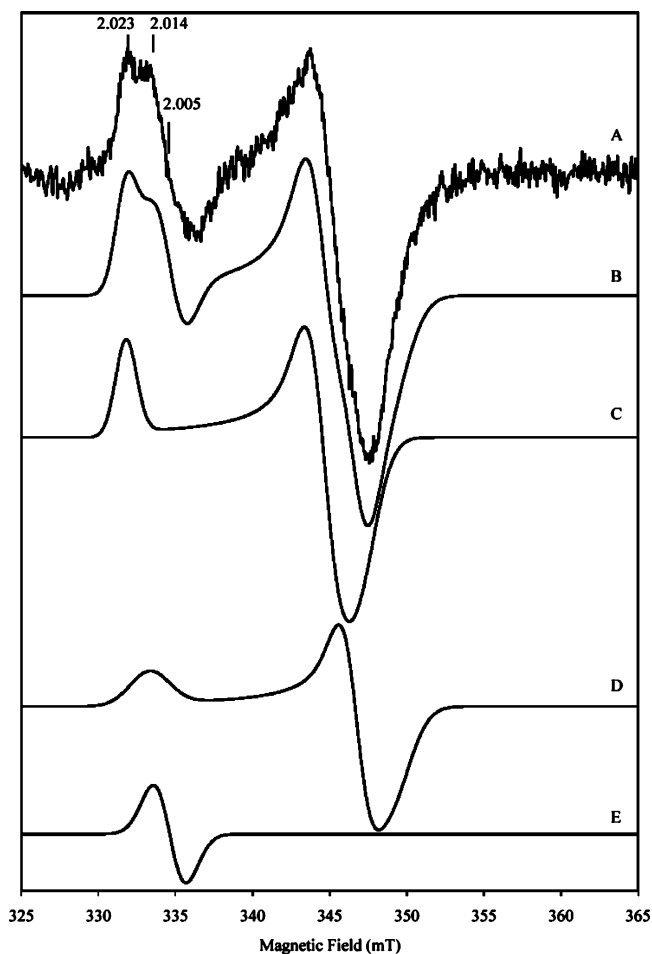


FIGURE 2: EPR spectrum of *R. marinus* complex I at 2.4 mW and 120 K, reduced with NADPH (A). Simulation of the total experimental spectrum (B) and different components used in the simulation,  $g$  values (line width in parentheses, in Gauss): 2.023 (16), 1.948 (22), 1.935 (28) (C), 2.014 (10), 1.936 (20), 1.923 (30) (D), and 2.005 (25) (E). (Microwave frequency: 9.36 GHz; modulation amplitude: 0.9 mT).

The fractions containing NADH dehydrogenase and NADH:quinone oxidoreductase activity, including the purified protein, were stored on ice in a cold chamber and concentrated in Diaflo or Centriplus from Amicon exclusively with YM100 membranes to avoid detergent concentration.

**Activity Assays.** NADH dehydrogenase activity was performed as in ref 18. NADH:quinone oxidoreductase activities were assayed anaerobically under argon at 55 °C following the oxidation of NADH at 330 nm ( $\epsilon = 5930 \text{ M}^{-1} \text{ cm}^{-1}$ ) and the reduction of dimethylnaphthoquinone (DMN) at 270 nm ( $\epsilon = 11\,687 \text{ M}^{-1} \text{ cm}^{-1}$ ). The reaction mixture contained 100 mM potassium phosphate buffer at pH 7.5, 0.1% DM, 50  $\mu\text{M}$  NADH, and 50  $\mu\text{M}$  DMN. The reaction was started by the addition of sample.

**EPR Spectroscopy.** EPR spectra were obtained as in ref 19, using 40  $\mu\text{M}$  of purified complex I. When cited, the sample was incubated with 10 mM NADH or 10 mM NADPH for 10 min at 50 °C. *R. marinus* membranes were incubated with 1 mM piericidin A for 5 min and reduced with NADH, NADPH, or succinate (10 mM each). The spectra obtained were theoretically simulated on the field space, using the dependence of the transition probability on the  $g$  values, as described by Aasa and Vanngard (20) and assuming homogeneously broadened Gaussian line widths.

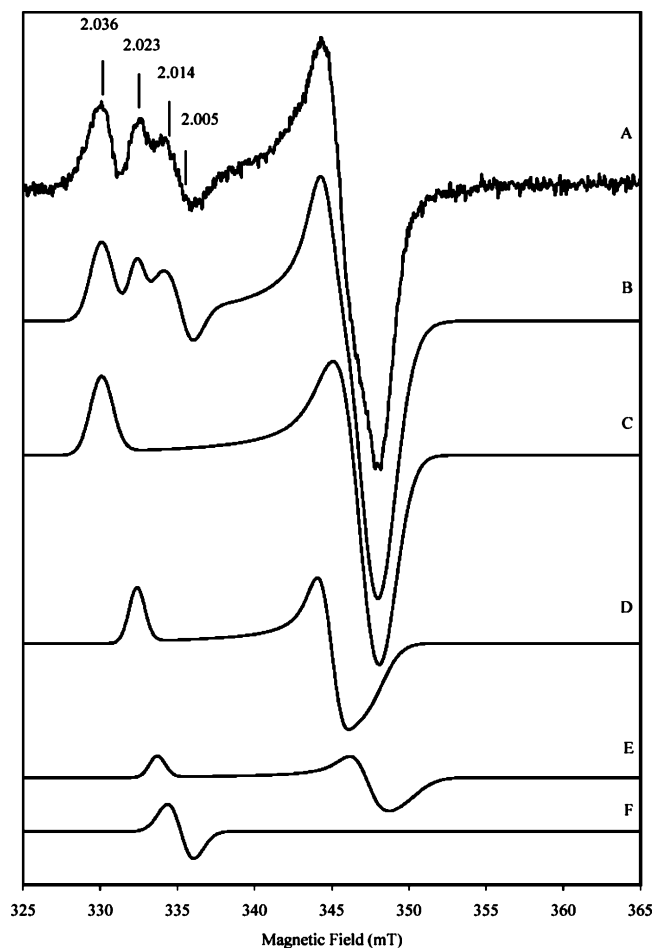


FIGURE 3: EPR spectrum of *R. marinus* complex I at 2.4 mW and 100 K, reduced with NADH (A). Microwave frequency: 9.36 GHz; modulation amplitude: 0.9 mT. Simulation of the experimental spectrum (B) and different components used in the simulation,  $g$  values (line width in parentheses, in Gauss): 2.036 (17), 1.938 (30), 1.932 (28) (C), 2.023 (12), 1.948 (16), 1.935 (28) (D), 2.014 (12), 1.936 (20), 1.923 (30) (E), and 2.005 (20) (F).

Anaerobic potentiometric titrations were followed by EPR spectroscopy at pH 7.5 and 20 °C, using 12  $\mu$ M of purified complex I and as redox mediators, each at a final concentration of 50  $\mu$ M: duroquinone, menadione, plumbagin, indigo trisulfonate, indigo disulfonate, phenazine, 2-hydroxy-1,4-naphthoquinone, anthraquinone-2-sulfonate, safranin, neutral red, benzyl viologen, and methyl viologen. The reduction potentials are quoted in relation to the standard hydrogen electrode. The Ag/AgCl and platinum electrodes were calibrated with quinhydrone.

## RESULTS

***R. marinus* Complex I Purification.** The *R. marinus* complex I purification by the described optimized methodology was revealed to be reproducible, with only one form of the complex being eluted from the last column, the Superdex 200, and the purified sample retained the NADH dehydrogenase activity over one month. Moreover, the turnovers of NADH oxidation and DMN reduction present a stoichiometry of 1:1, which reflects the integrity of the complex.

No activity was detected in this preparation when NADPH is the electron donor, similarly to what happened when the previous purification methods were used.

**EPR Studies.** Figure 1 shows EPR spectra of *R. marinus* membranes incubated with piericidin A and reduced with

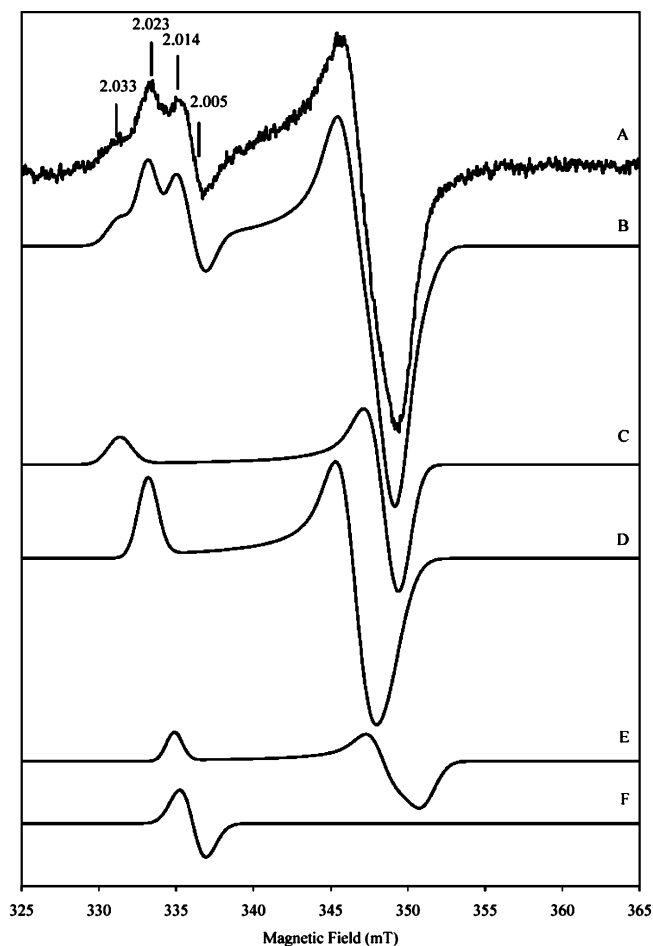


FIGURE 4: EPR spectrum of *R. marinus* complex I at 2.4 mW and 65 K, reduced with 10 mM NADH (A). Microwave frequency: 9.36 GHz; modulation amplitude: 0.9 mT. Simulation of the experimental spectrum (B) and different components used in the simulation,  $g$  values (line width in parentheses, in Gauss): 2.033 (18), 1.937 (20), 1.930 (18) (C), 2.023 (15), 1.948 (25), 1.935 (27) (D), 2.014 (12), 1.936 (20), 1.923 (20) (E), and 2.005 (20) (F).

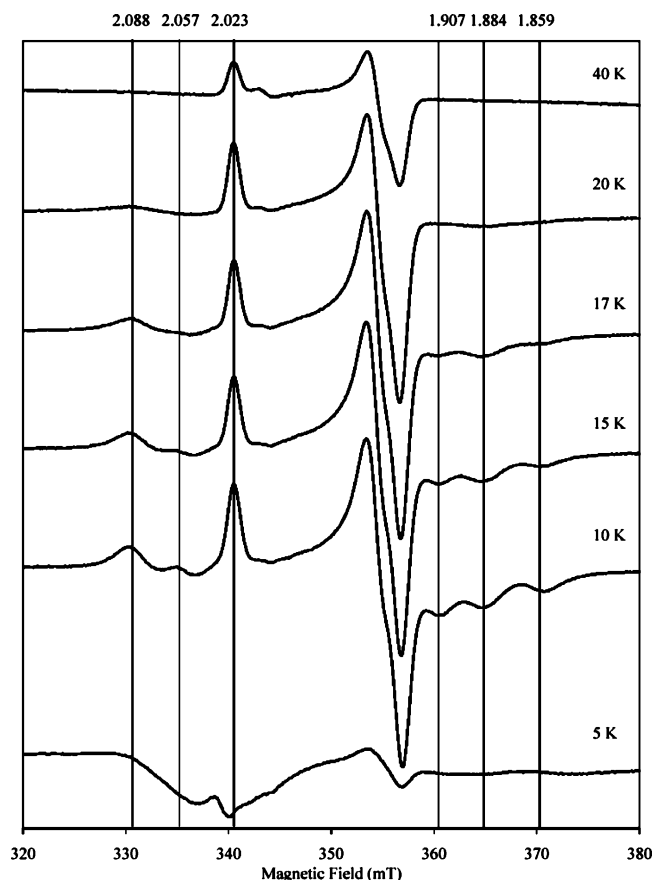
NADH, NADPH, or succinate. The observed EPR signals in the first two conditions are due to complex I components with the exception of the signal with  $g = 2.03$  attributed to the S3 center of succinate:quinone oxidoreductase (Figure 1A,B) (21). Upon reduction of the previously piericidin A incubated membranes with succinate (Figure 1C) center S3 is not completely reduced, and thus its EPR signal is still observed, although less intense. Apart from center S3, in these conditions only resonances attributed to center S1 are observed (21). The resonances of S1 are not present in the spectra of the membranes reduced with NADH or NADPH (Figure 1A,B).

Spectra of the purified *R. marinus* NADH:quinone oxidoreductase reduced with NADH, NADPH, NADH plus dithionite, and NADPH plus dithionite were obtained at different temperatures and microwave powers (Figures 2–9). In the oxidized state *R. marinus* NADH:quinone oxidoreductase does not present any EPR signal.

**EPR Spectra Obtained at High Temperature.** Figure 2 shows the EPR spectrum of *R. marinus* NADH:quinone oxidoreductase reduced with NADPH plus dithionite at 120 K and 2.4 mW. Three different signals can be deconvoluted, with  $g$  values at 2.023, 1.948, 1.935; 2.014, 1.936, 1.923, and 2.005, corresponding to a radical. The assignment of

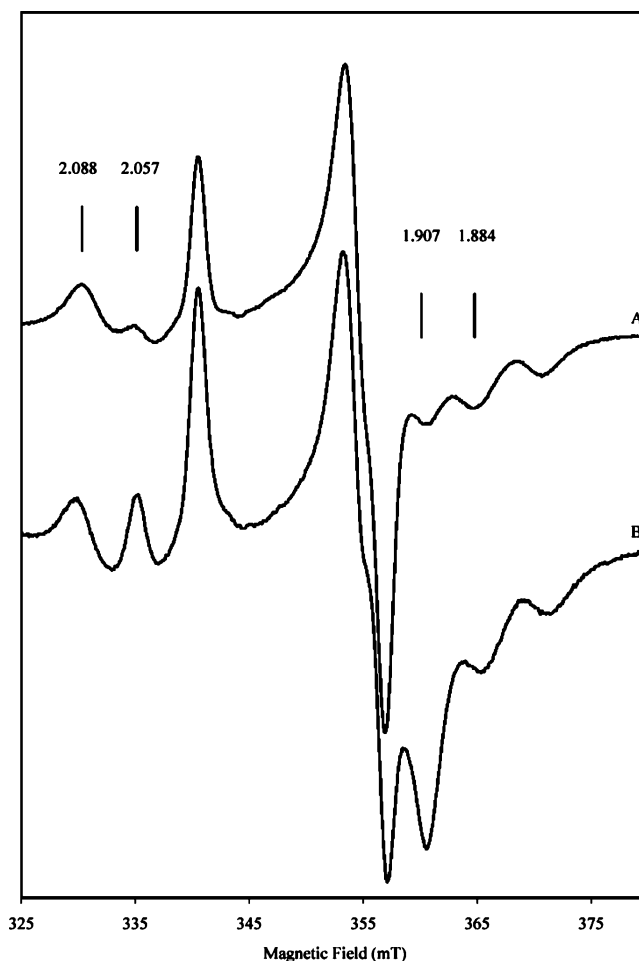
Table 1: Iron–Sulfur Centers Detected by EPR Spectroscopy in *R. marinus* Complex I and Respective Reduction Potentials

center type	assignment	$g_{\max}$	$g_{\text{med}}$	$g_{\min}$	$E^\circ$ (mV)
[2Fe-2S] <sup>2+/1+</sup>	N1a	2.023	1.948	1.935	–240
[2Fe-2S] <sup>2+/1+</sup>		2.014	1.936	1.923	
[2Fe-2S] <sup>2+/1+</sup>		2.036	1.938	1.932	
[2Fe-2S] <sup>2+/1+</sup>		2.033	1.937	1.932	
[4Fe-4S] <sup>2+/1+</sup>	N5	2.020	1.919	1.847	–240
[4Fe-4S] <sup>2+/1+</sup>	N3	2.033	1.918	1.859	–240
[4Fe-4S] <sup>2+/1+</sup>	N2	2.057	1.920	1.907	< –450
[4Fe-4S] <sup>2+/1+</sup>	N4	2.088	1.930	1.884	–240

FIGURE 5: EPR spectra of *R. marinus* purified complex I at 2.4 mW reduced with 10 mM NADH plus excess of dithionite at different temperatures. Microwave frequency: 9.64 GHz; modulation amplitude: 0.9 mT.

the different components of each rhombic signal was based on the spectrum obtained at 40 K of the NADH reduced sample (Figure 5) (see below, where the main signal presents  $g$  values of 2.023, 1.948, 1.935). The possible presence of another center with  $g_{\max}$  at 2.033 in this spectrum, although not excluded, is not certain due to its very low intensity and thus was not included in the simulation. Apart from the resonance assigned to a radical, those observed at these high temperatures are due to reduced binuclear iron–sulfur centers.

The EPR signals observed at the above-mentioned conditions are also observed in the spectra of the sample reduced with NADH plus dithionite obtained at 120 K (not shown) and 100 K (Figure 3). In this case another binuclear iron–sulfur center with  $g$  values of 2.036, 1.938, and 1.932 is also distinctly observed (Figure 3C), but it was not reproduced in all preparations, which questions its assignment to another center. The simulation of the spectrum of the sample reduced

FIGURE 6: EPR spectra of *R. marinus* complex I reduced with 10 mM NADH (A) and NADH plus excess of dithionite (B) at 10 K and 2.4 mW. Microwave frequency: 9.64 GHz; modulation amplitude: 0.9 mT.

with NADH plus dithionite obtained at 100 K is presented in Figure 3, which shows three signals assigned to binuclear iron–sulfur centers and the presence of a radical.

In Figure 4 is shown the spectrum of the sample reduced with NADH, obtained at 65 K. Here four different signals can also be deconvoluted. Two with  $g$  values at 2.023, 1.948, 1.935 (Figure 4D) and 2.014, 1.936, 1.923 (Figure 4E) correspond to the binuclear iron–sulfur centers, and one with a  $g$  value at 2.005 (Figure 4F) corresponds to the radical observed at 100/120 K. A third binuclear iron–sulfur species has  $g$  values at 2.033, 1.937, and 1.932 (Figure 4C). This center can be the same one suspected also to be present in the spectrum of the enzyme reduced with NADPH plus dithionite at 120 K, and the hypothesis cannot be excluded that it is also the same one observed at 100 K upon reduction with NADH plus dithionite.

Overall, from the EPR spectra of *R. marinus* NADH: quinone oxidoreductase obtained at high temperatures, it can be concluded that certainly two, but up to four, binuclear iron–sulfur centers may be present in the complex (see below, Table 1).

**EPR Spectra at Low Temperatures.** The spectrum of the sample reduced with NADH, obtained at 20 K (Figure 5) is dominated by the resonances attributed to the binuclear center with  $g$  values at 2.023, 1.948, 1.935. A new signal develops with  $g_{\max}$  at 2.088 and  $g_{\min}$  at 1.884, which is better observed

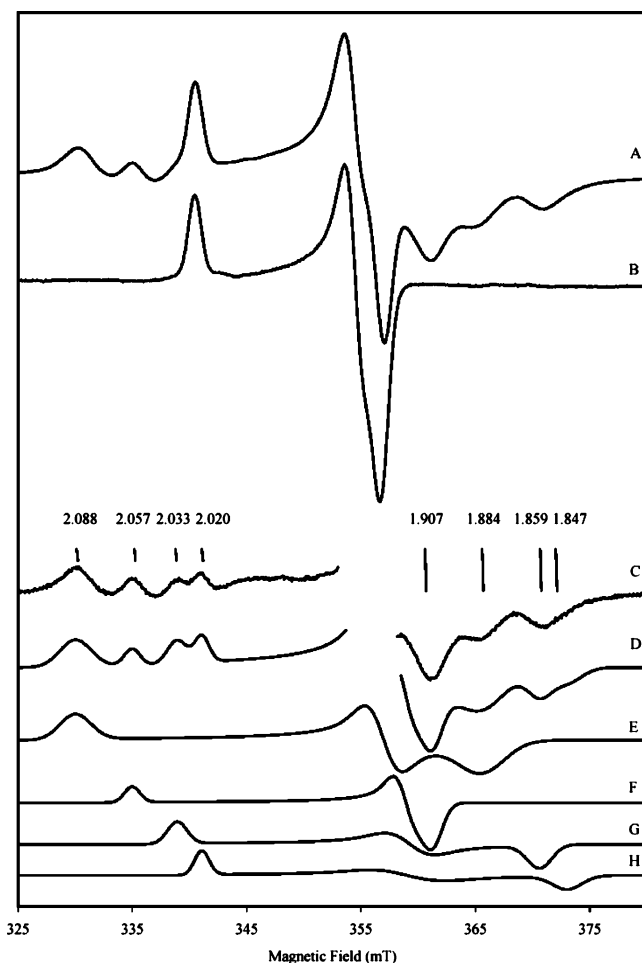


FIGURE 7: EPR spectra of *R. marinus* complex I reduced with 10 mM NADPH, at 24 mW, at 10 K (A) and at 40 K (B). Microwave frequency: 9.64 GHz; modulation amplitude: 0.9 mT. A minus B (C). Simulation of the spectral subtraction (D) and different components used in the simulation,  $g$  values: 2.088, 1.930, 1.884 (E), 2.057, 1.920, 1.907 (F), 2.033, 1.918, 1.859 (G), 2.020, 1.919, 1.847 (H).

at lower temperatures (Figure 5).

Comparison of the spectra obtained at 10 K of the NADH and NADH plus dithionite reduced samples (Figure 6) indicates an increase in the intensity of the signal with  $g_{\max} = 2.057$  and  $g_{\min} = 1.907$ , thus allowing the assignment of these two  $g$  values to the same center.

In the spectrum obtained at 10 K of the sample reduced with NADH plus dithionite, two other  $g_{\min}$  values in the region of 1.85 are observed (Figure 5). Subtractions of spectra obtained at different conditions allowed the observation of the  $g_{\max}$  counterparts. Figure 7C shows a subtraction of the spectrum of the NADPH reduced sample obtained at 10 K, 24 mW (Figure 7A) minus the one obtained at 40 K, 24 mW (Figure 7B). The assignment of each  $g_{\max}$  to the corresponding  $g_{\min}$  was facilitated by the spectra obtained at 6.5 K (Figure 8). Although most of the centers are saturated at this temperature, the comparison of the spectra obtained at different microwave powers allows correlation of  $g_{\max} = 2.033$  with  $g_{\min} = 1.859$  and  $g_{\max} = 2.020$  with  $g_{\min} = 1.847$ .

From the spectra at low temperature, it can be concluded that four tetranuclear iron-sulfur centers are present (Table 1).

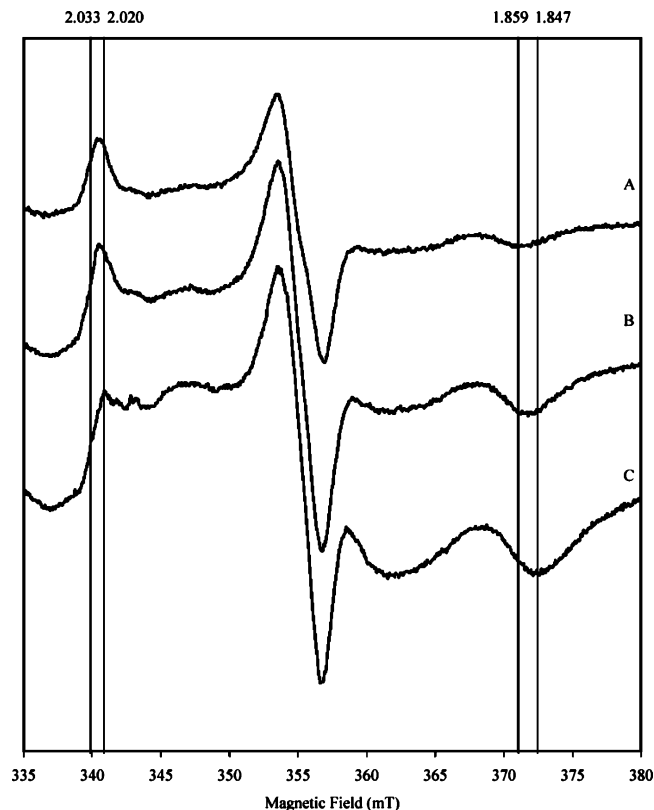


FIGURE 8: EPR spectra of *R. marinus* complex I reduced with 10 mM NADH at 6.5 K and 0.24 (A), 2.4 (B), and 24 mW (C). Microwave frequency: 9.64 GHz; modulation amplitude: 0.9 mT.

An accurate deconvolution of the different  $g_{\text{med}}$  was not possible because these have values very close together. Those values were attributed to each signal to have a good overall fit.

Considering these spectral deconvolutions, the spectrum of the *R. marinus* NADH:quinone oxidoreductase reduced with NADH plus dithionite obtained at 10 K and 24 mW could be simulated with five different components (Figure 9).

**Redox Titration.** The reduction potentials of the different iron-sulfur centers were determined by redox titrations monitored by EPR. Each sample was measured at different temperatures. Figure 10 shows the reduction behavior of the several EPR signals. With the exception of the iron-sulfur center with  $g$  values at 2.057 and 1.907, all the centers seem to have roughly the same reduction potential of  $-240 \pm 20$  mV (Table 1). The iron-sulfur center with  $g_{\max} = 2.057$  and  $g_{\min} = 1.907$  could not be fully reduced with the used experimental conditions. By normalizing its EPR signal intensity to the one obtained in the spectrum shown in Figure 9, it can be estimated that ca. 20% of the center was reduced. This behavior can be described by a Nernst curve with a reduction potential of  $\sim -450$  mV. This value is very approximate; it can only be concluded that the center with a  $g_{\max}$  at 2.057 has a reduction potential much lower than the other iron-sulfur centers present in *R. marinus* complex I. This is in agreement with the observations that this low reduction potential center can be completely reduced in the presence of NADH or NADPH only when dithionite is added to the preparation.

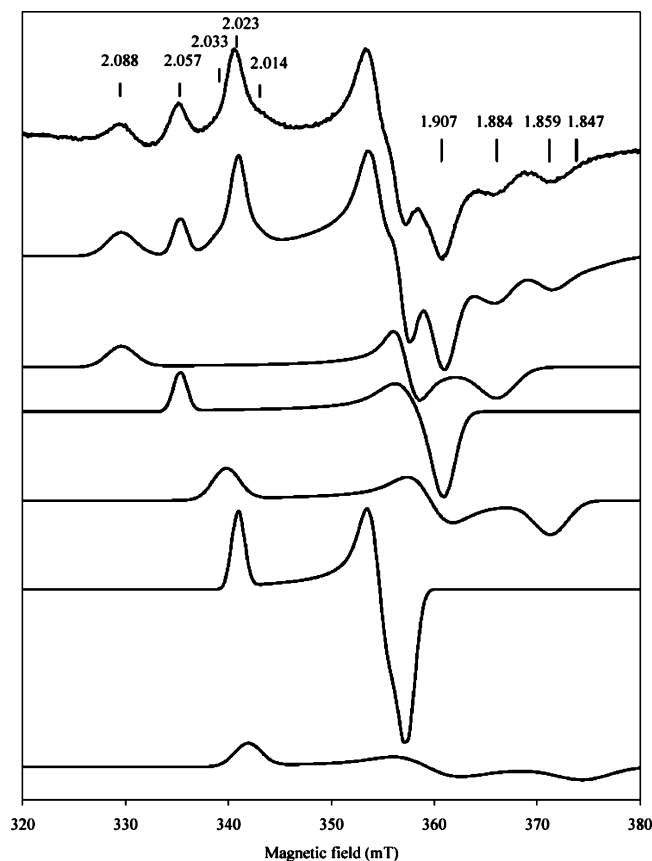


FIGURE 9: EPR spectrum of *R. marinus* complex I reduced with 10 mM NADH plus dithionite, at 10 K and 2.4 mW (A), simulation of the experimental spectrum (B), and different components used in the simulation,  $g$  values: 2.088, 1.930, 1.884 (C), 2.057, 1.920, 1.907 (D), 2.033, 1.918, 1.859 (E), 2.023, 1.948, 1.935 (F), 2.020, 1.919, 1.847 (G).

## DISCUSSION

Depending on the organism, 8–10 canonical, iron–sulfur centers binding sites may be present in the amino acid sequences of complex I subunits. However, only five or six iron–sulfur centers have been detected by EPR in an intact complex; the other centers were detected only in individually expressed subunits. According to their relaxation properties in the mitochondrial complex, they were named N1a, N1b, N2, N3, N4, N5, N6a, and N6b by Ohnishi (7, 13, 22). In *E. coli* and *T. thermophilus* complex I, another center was observed by EPR (in agreement with their amino acid sequence) and later shown to be a  $[4\text{Fe-4S}]^{2+/1+}$  center. This is now referred to as N7, and recently its presence was confirmed by X-ray analysis (6). A 10th putative binding site is present in the amino acid sequences of some other complexes, as for example in the one from *Helicobacter pylori* (sequenced genome).

The EPR data on *R. marinus* NADH:quinone oxidoreductase revealed the unequivocal presence of two  $[2\text{Fe-2S}]^{2+/1+}$  and four  $[4\text{Fe-4S}]^{2+/1+}$  centers (Table 1). On the basis of observations of the spectra obtained at high temperatures, the presence of up to two more  $[2\text{Fe-2S}]^{2+/1+}$  centers may be considered. The spectral deconvolution here performed was made on the assumption that interactions among the different iron–sulfur centers are absent. Although there is no clear evidence for such an interaction, it cannot be excluded because, as expected and shown in the X-ray

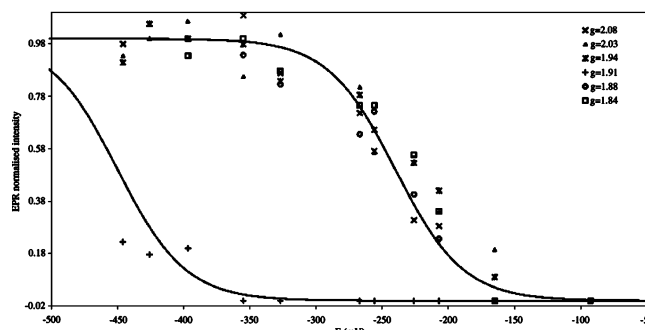
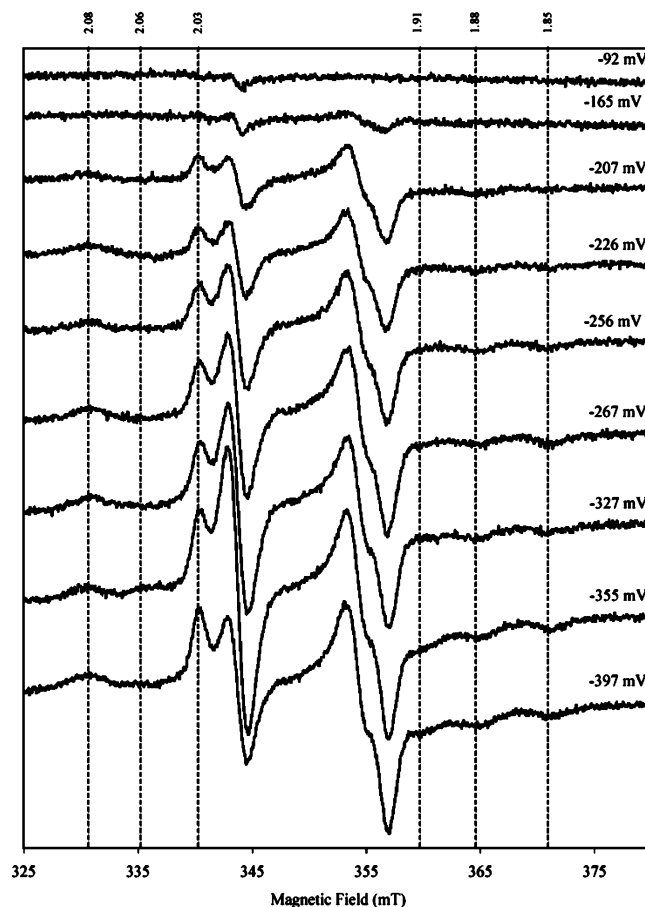


FIGURE 10: *R. marinus* complex I titration followed by EPR (2.4 mW, 10 K). Microwave frequency: 9.64 GHz; modulation amplitude: 0.9 mT (top). The changes in EPR intensity were monitored at  $g$  values: 2.088, 2.023, 1.948, 1.907, 1.884, and 1.859/1.847 (see legend) (bottom). The reduction behavior of these species with the exception of the components with  $g$  values at 2.057 and 1.907 are described by a Nernst curve with a reduction potential of  $-240 \pm 10$  mV. The components with  $g$  values at 2.057 and 1.907 are described by a Nernst curve with a reduction potential of  $-450$  mV. See text.

analysis of the iron–sulfur centers of complex I from *T. thermophilus*, the centers are in close proximity, arranged with edge-to-edge distances between 9 and 14 Å. The observed centers were tentatively named according to the currently used nomenclature by comparing their  $g$  values with the ones found in the bovine enzyme (7) (Table 1): due to their  $g$  values the centers with  $g_{\text{max}}$  at 2.088 and 2.057 may correspond to N4 and N2, respectively; the  $g_{\text{max}} = 2.033$  may correspond to N3, and this may be corroborated by the fact that the signal with  $g_{\text{max}} = 2.020$  is the one with fastest relaxation properties and thus being assigned to N5. By doing this assignment, it results that *R. marinus* center N2 is the

one with the lowest reduction potential in this complex ( $< -450$  mV), being that all the other centers, including center N1a, have isopotentials at  $\sim -240$  mV. However, the actual potential of each center may not be critical, i.e., they may serve mainly as a way of ensuring electron transfer from the donor to the acceptor like, as observed, for example, in succinate:quinone oxidoreductases or in bacterial hydrogenases (23).

In the subunit amino acid sequences of *R. marinus* complex I, the eight conserved iron–sulfur binding sites are present and the referred extra binding site for N7 is absent (17). This is compatible with the observed EPR resonances due to two  $[2\text{Fe-2S}]^{2+/1+}$  and four  $[4\text{Fe-4S}]^{2+/1+}$ , described in the present work. The other two possible observed EPR resonances at high temperatures and thus assigned to  $[2\text{Fe-2S}]^{2+/1+}$  centers may be due to centers without canonical binding sites, to protein heterogeneity, or to interactions among the different iron–sulfur centers.

In conclusion, in the intact complex I from *R. marinus* two binuclear and four tetranuclear iron–sulfur centers were unequivocally observed by EPR spectroscopy. Up to two more binuclear centers may also be present in the complex. Their redox properties were analyzed, and it was observed that the centers, with the exception of N2, have a reduction potential of  $-240$  mV. Center N2 unusually presents a much lower reduction potential  $< -450$  mV.

## ACKNOWLEDGMENT

João Carita performed *Rhodothermus marinus* growth. A.S.F. and M.M.P. are recipients of grants from Praxis XXI program (BPD/16388/2004 and BPD/11621/2002).

## REFERENCES

1. Guenebaut, V., Vincentelli, R., Mills, D., Weiss, H., and Leonard, K. R. (1997) Three-dimensional structure of NADH-dehydrogenase from *Neurospora crassa* by electron microscopy and conical tilt reconstruction, *J. Mol. Biol.* 265, 409–418.
2. Djafarzadeh, R., Kerscher, S., Zwickler, K., Radermacher, M., Lindahl, M., Schagger, H., and Brandt, U. (2000) Biophysical and structural characterization of proton-translocating NADH-dehydrogenase (complex I) from the strictly aerobic yeast *Yarrowia lipolytica*, *Biochim. Biophys. Acta* 1459, 230–238.
3. Grigorieff, N. (1998) Three-dimensional structure of bovine NADH:ubiquinone oxidoreductase (complex I) at 22 Å in ice, *J. Mol. Biol.* 277, 1033–1046.
4. Peng, G., Fritsch, G., Zickermann, V., Schagger, H., Mentele, R., Lottspeich, F., Bostina, M., Radermacher, M., Huber, R., Stetter, K. O., and Michel, H. (2003) Isolation, characterization and electron microscopic single particle analysis of the NADH:ubiquinone oxidoreductase (complex I) from the hyperthermophilic eubacterium *Aquifex aeolicus*, *Biochemistry* 42, 3032–3039.
5. Guenebaut, V., Schlitt, A., Weiss, H., Leonard, K., and Friedrich, T. (1998) Consistent structure between bacterial and mitochondrial NADH:ubiquinone oxidoreductase (complex I), *J. Mol. Biol.* 276, 105–112.
6. Hinchliffe, P., and Sazanov, L. A. (2005) Organization of iron–sulfur clusters in respiratory complex I, *Science* 309, 771–774.
7. Ohnishi, T. (1998) Iron–sulfur clusters/semiquinones in complex I, *Biochim. Biophys. Acta* 1364, 186–206.
8. Nakamaru-Ogiso, E., Yano, T., Ohnishi, T., and Yagi, T. (2002) Characterization of the iron–sulfur cluster coordinated by a cysteine cluster motif (CXXCXXCX27C) in the Nqo3 subunit in the proton-translocating NADH-quinone oxidoreductase (NDH-1) of *Thermus thermophilus* HB-8, *J. Biol. Chem.* 277, 1680–1688.
9. Uhlmann, M., and Friedrich, T. (2005) EPR signals assigned to Fe/S cluster N1c of the *Escherichia coli* NADH:ubiquinone oxidoreductase (complex I) derive from cluster N1a, *Biochemistry* 44, 1653–1658.
10. Friedrich, T. (1998) The NADH:ubiquinone oxidoreductase (complex I) from *Escherichia coli*, *Biochim. Biophys. Acta* 1364, 134–146.
11. Sled, V. D., Friedrich, T., Leif, H., Weiss, H., Meinhardt, S. W., Fukumori, Y., Calhoun, M. W., Gennis, R. B., and Ohnishi, T. (1993) Bacterial NADH-quinone oxidoreductases: iron–sulfur clusters and related problems, *J. Bioenerg. Biomembr.* 25, 347–356.
12. Meinhardt, S. W., Wang, D. C., Hon-nami, K., Yagi, T., Oshima, T., and Ohnishi, T. (1990) Studies on the NADH-menaquinone oxidoreductase segment of the respiratory chain in *Thermus thermophilus* HB-8, *J. Biol. Chem.* 265, 1360–1368.
13. Meinhardt, S. W., Kula, T., Yagi, T., Lillich, T., and Ohnishi, T. (1987) EPR characterization of the iron–sulfur clusters in the NADH: ubiquinone oxidoreductase segment of the respiratory chain in *Paracoccus denitrificans*, *J. Biol. Chem.* 262, 9147–9153.
14. Rasmussen, T., Scheide, D., Brors, B., Kintscher, L., Weiss, H., and Friedrich, T. (2001) Identification of two tetranuclear FeS clusters on the ferredoxin-type subunit of NADH:ubiquinone oxidoreductase (complex I), *Biochemistry* 40, 6124–6131.
15. Wang, D. C., Meinhardt, S. W., Sackmann, U., Weiss, H., and Ohnishi, T. (1991) The iron–sulfur clusters in the two related forms of mitochondrial NADH: ubiquinone oxidoreductase made by *Neurospora crassa*, *Eur. J. Biochem.* 197, 257–264.
16. Dupuis, A., Chevallet, M., Darrouzet, E., Duborjal, H., Lunardi, J., and Issartel, J. P. (1998) The complex I from *Rhodobacter capsulatus*, *Biochim. Biophys. Acta* 1364, 147–165.
17. Melo, A. M., Lobo, S. A., Sousa, F. L., Fernandes, A. S., Pereira, M. M., Hreggvidsson, G. O., Kristjansson, J. K., Saraiva, L. M., and Teixeira, M. (2005) A nhaD Na<sup>+</sup>/H<sup>+</sup> antiporter and a pcD homologues are among the *Rhodothermus marinus* complex I genes, *Biochim. Biophys. Acta* 1709, 95–103.
18. Fernandes, A. S., Pereira, M. M., and Teixeira, M. (2002) Purification and characterization of the complex I from the respiratory chain of *Rhodothermus marinus*, *J. Bioenerg. Biomembr.* 34, 413–421.
19. Pereira, M. M., Carita, J. N., and Teixeira, M. (1999) Membrane-bound electron-transfer chain of the thermohalophilic bacterium *Rhodothermus marinus*: a novel multi-hemic cytochrome bc<sub>1</sub> a new complex III, *Biochemistry* 38, 1268–1275.
20. Aasa, R., and Vänngård, V. T. (1975) EPR signal intensity and powder shapes: A reexamination, *J. Magn. Res.* 19, 308–315.
21. Fernandes, A. S., Pereira, M. M., and Teixeira, M. (2001) The succinate dehydrogenase from the thermohalophilic bacterium *Rhodothermus marinus*: redox-Bohr effect on heme bL, *J. Bioenerg. Biomembr.* 33, 343–352.
22. Yano, T., Magnitsky, S., Sled, V. D., Ohnishi, T., and Yagi, T. (1999) Characterization of the putative 2x[4Fe-4S]-binding NQO9 subunit of the proton-translocating NADH-quinone oxidoreductase (NDH-1) of *Paracoccus denitrificans*. Expression, reconstitution, and EPR characterization, *J. Biol. Chem.* 274, 28598–28605.
23. Page, C. C., Moser, C. C., and Dutton, P. L. (2003) Mechanism for electron transfer within and between proteins, *Curr. Opin. Chem. Biol.* 7, 551–556.

BI0519452